JURNAL INFOTEL
VOL. 18, NO. 1, FEBRUARY 2026, PP. 59–76. DOI:10.20895/INFOTEL.V18I1.1325

RESEARCH ARTICLE

Comparative Analysis of Grey Wolf Optimizer-based MPPT System with SEPIC Converter for Stand-Alone PV Applications

Riny Sulistyowati[1,*] and Wildan Agung Pambudi[2]

[1,2]Department of Electrical Engineering, Adhi Tama Institute of Technology Surabaya, 60117, Indonesia

*Corresponding email: riny.971073@itats.ac.id

Received: February 05, 2025; Revised: December 05, 2025; Accepted: February 08, 2026.

Abstract: This paper presents a comprehensive investigation into the design and evaluation of a Grey Wolf Optimizer (GWO)-based Maximum Power Point Tracking (MPPT) system integrated with a Single-Ended Primary Inductor Converter (SEPIC) for stand-alone Photovoltaic (PV) systems. The study aims to assess the optimization performance of the GWO algorithm in comparison with conventional MPPT methods. The hardware-based design of the SEPIC converter achieves an average efficiency of 62.45%, with a controlled error margin of 15.26% and a remarkable output voltage stability of 5 mV. The GWO Algorithm is tailored to pinpoint the optimal operating point of the solar panel, yielding a superior power extraction accuracy of 99% and agile tracking with a speed of 2 ms under ideal conditions and 140 ms under non-ideal conditions. The simulation results demonstrate the ability of GWO to generate up to 2 watts more optimal power than traditional algorithms, in both ideal and non-ideal scenarios. Real-world field tests validate the GWO algorithm's accelerated convergence, increased robustness, and unwavering stability under diverse environmental conditions.

Keywords: Grey Wolf Optimizer (GWO), Maximum Power Point Tracking (MPPT), Power Extraction Efficiency, Stand-Alone PV System, SEPIC Converter

 ISSN: 2085-3688; e-ISSN: 2460-0997

1 Introduction

The growing interest in Photovoltaic (PV) systems is largely due to their ability to harness solar energy for power generation. These systems are increasingly recognized for their potential to provide sustainable energy solutions, particularly as the world moves towards renewable energy sources. However, the efficiency of PV systems is highly dependent on consistent solar irradiance and temperature levels, leading to varying Maximum Power Points (MPP) throughout the day [1] To maximize energy output, PV arrays must operate at voltages corresponding to the MPP. This is achieved through Maximum Power Point Tracking (MPPT), which is a critical component in the optimization of energy generation systems.

The implementation of MPPT not only enhances energy production, but also reduces the costs associated with the construction and maintenance of the photovoltaic system. By integrating MPPT, control systems become more responsive, allowing for rapid adaptation to changing weather conditions and load variations, which are common challenges in PV applications. Various MPPT techniques have been developed, the most common being the Incremental Conductance (IC) and Perturb and Observe (PnO) methods [2–6]. Although these conventional techniques are effective, they exhibit limitations, such as a sluggish response to rapid changes in irradiance and susceptibility to oscillations around the MPP [7].

In recent years, the Grey Wolf Optimizer (GWO) method has emerged as a powerful metaheuristic algorithm inspired by the social and hunting behavior of North American gray wolves. GWO has demonstrated robust optimization capabilities and has been successfully applied in various engineering fields, including MPPT algorithms for PV systems [8]. Its application has been extended to battery energy storage systems, optimal design of synchronous magnet motors, and power flow optimization solutions [9–12]. Research comparing GWO with other optimization algorithms, such as Particle Swarm Optimization (PSO), has shown GWO's superiority in terms of convergence speed, centralization of solutions, and overall optimization accuracy [13, 14]. The selection of the appropriate converter topology is crucial for the success of the MPPT system in photovoltaic applications. The chosen topology must be capable of efficiently boosting or buckling the voltage while achieving high voltage gain. Among the commonly used topologies, the Buck-Boost converter and the SEPIC converter stand out for their versatility and efficiency [15, 16]. In this research, the SEPIC converter was chosen due to its higher efficiency compared to other DC-DC converters, making it an ideal choice for MPPT applications [17, 18].

This study aims to design a GWO-based MPPT system using a SEPIC converter for a stand-alone PV system. The performance of the GWO algorithm is compared with that of the PnO and Hill Climbing (HC) algorithms to determine the most effective optimization technique. The research begins with separate setups for the control system (GWO algorithm) and the SEPIC converter to analyze their individual performances. The SEPIC converter's efficiency is compared against CuK and Buck-Boost converters, while the GWO algorithm's optimization capabilities are evaluated against PnO and HC methods. Finally, the entire MPPT system is integrated and tested under various conditions, including different irradiance levels and partially shaded conditions, to evaluate its performance in real-world scenarios.

2 Research Method

2.1 MPPT Control and Monitoring System

The Maximum Power Point Tracker (MPPT) optimizes the power output of a photovoltaic (PV) generator [12,19]. The MPPT system comprises a DC-DC converter, which is essential to maximize the converter's efficiency. The general implementation of the system, including the integration of various components, is shown in Figure 1.

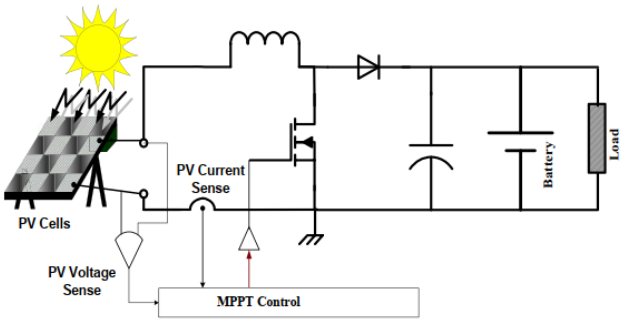

Figure 1: MPPT system overview.

In the MPPT control system, the duty cycle of the DC-DC converter is regulated to maintain operation at the Maximum Power Point (MPP). This control is achieved through a Microcontroller (MCU) that implements different MPPT algorithms, including Perturb and Observe (P&O) and Incremental Conductance (IC). The implementation of these algorithms is illustrated in Figure 2.

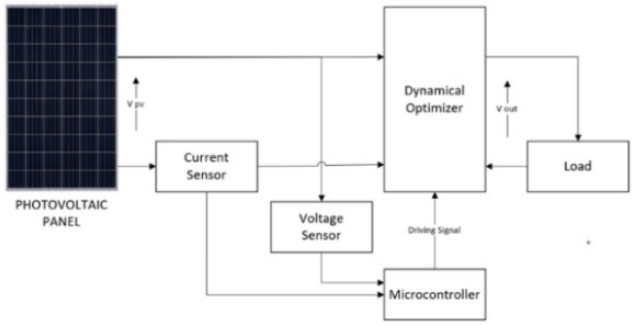

Figure 2: MPPT system implementation with microcontroller.

The hardware design for the MPPT system includes several components: a solar panel, SEPIC converter, MPPT control and monitoring circuit, sensor circuit, and load. The integration of these components into the MPPT system is shown in Figure 3.

The MPPT control system utilizes an Arduino Due Microcontroller connected to various sensors and peripherals. Figure 4 shows the MPPT control configuration.

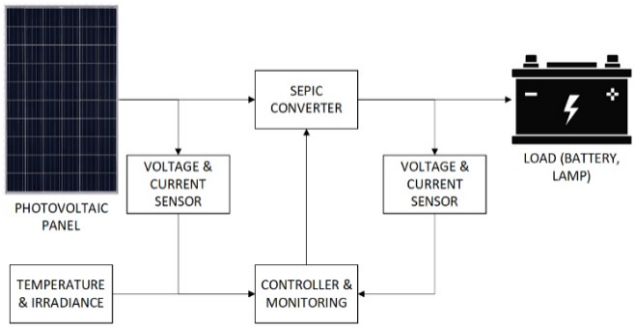

Figure 3: MPPT system implementation with microcontroller.

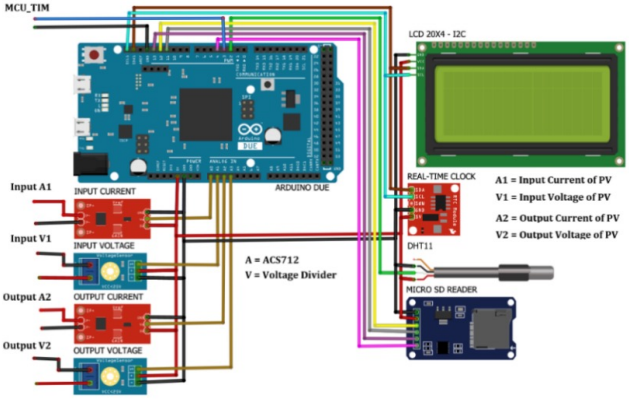

Figure 4: MPPT control configuration with microcontroller and sensors.

The MPPT Control System code is written in C and is uploaded to the Arduino interface. Using the Grey Wolf Optimizer (GWO) algorithm, it mimics the hunting behavior of gray wolves [8]. The algorithm's stages include Tracking, Encircling, Attacking (Exploitation), and Searching (Exploration), as outlined in Figure 5.

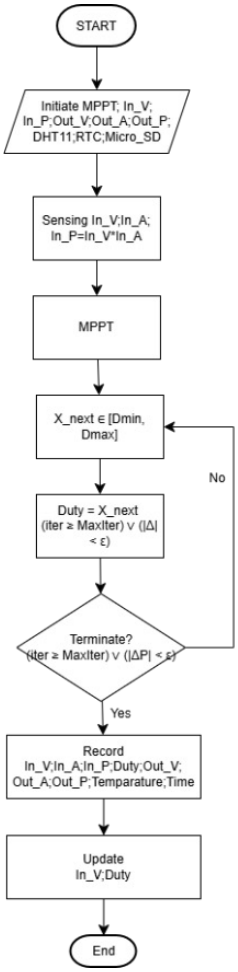

Figure 5: MPPT control system code flowchart.

2.2 SEPIC Converter

The single end primary inductor converter (SEPIC) is a DC-DC converter capable of producing an output voltage that can be higher or lower than the input voltage [17]. The topology of the SEPIC converter and its switching waveforms are shown in Figure 6 and Figure 7.

The parameters of the SEPIC converter are crucial for its performance. These parameters are determined using the following equations.

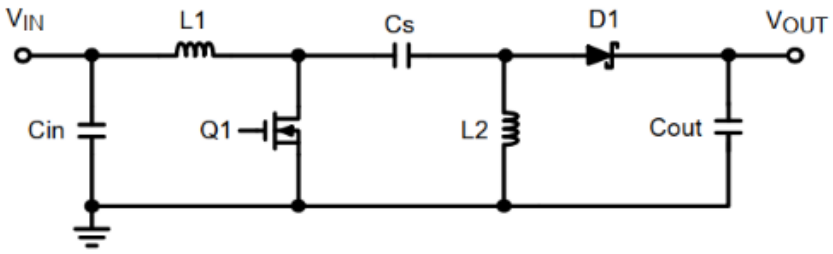

Figure 6: SEPIC DC converter topology.

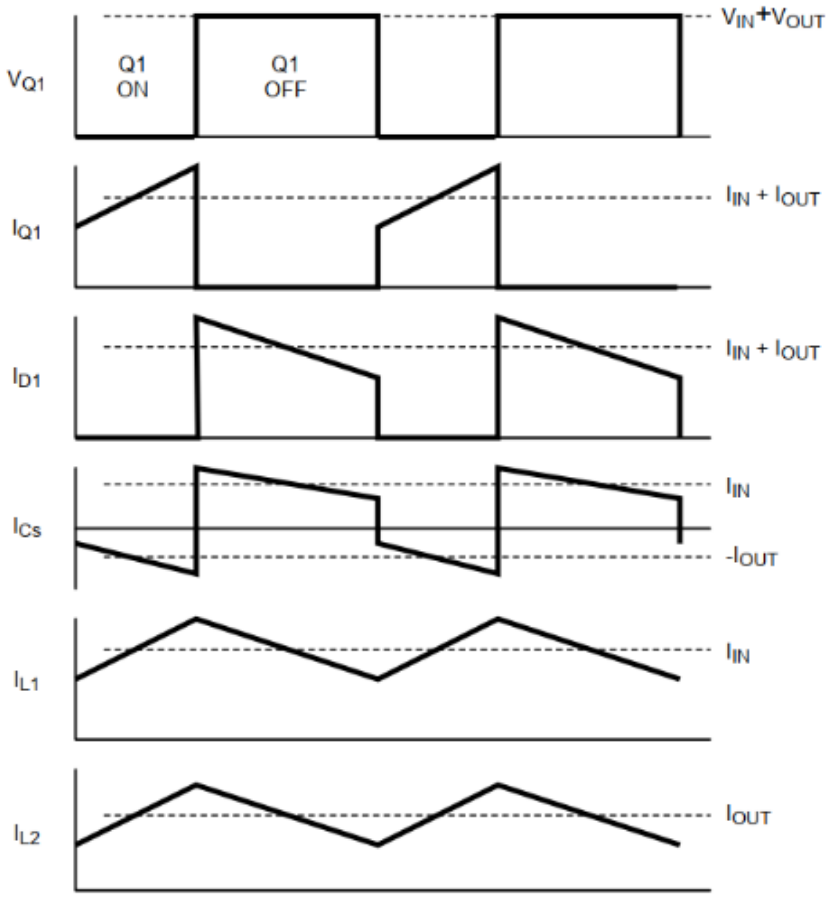

Figure 7: SEPIC switching waveform.

1. Duty Cycle Calculation

$$D = \frac{V_{\text{out}} + V_D}{V_{\text{in}} + V_{\text{out}} + V_D} \tag{1}$$

2. Maximum Duty Cycle

$$D_{\max} = \frac{V_{\text{out}} + V_D}{V_{\text{in(min)}} + V_{\text{out}} + V_D} \tag{2}$$

3. Minimum Duty Cycle

$$D_{\min} = \frac{V_{\text{out}} + V_D}{V_{\text{in(max)}} + V_{\text{out}} + V_D} \tag{3}$$

4. Inductor Current Ripple

$$\Delta I_L = I_{\text{in}} \times 40\% = I_{\text{out}} \times \frac{V_{\text{out}}}{V_{\text{in}}} \times 40\% \tag{4}$$

5. Inductor Value (L1 and L2)

$$L1 = L2 = L = \frac{V_{\text{in(min)}}}{\Delta I_L \times f_{\text{sw}}} \times D_{\max} \tag{5}$$

6. Series Capacitor Value

$$C_S = \frac{I_{\text{out}} \times D_{\max}}{\Delta V_{C_S} \times f_{\text{sw}}} \tag{6}$$

7. Output Capacitor Value

$$C_{\text{out}} \geq \frac{I_{\text{out}} \times D}{V_{\text{ripple}} \times 0.5 \times f_{\text{sw}}} \tag{7}$$

8. Input Capacitor Value

$$C_{\text{in}} = \frac{I_{\text{in(max)}} \times T}{\Delta V} \tag{8}$$

Table 1: SEPIC converter specifications

Parameter	**Value**
Input Voltage (V_{in})	12 V - 18.3 V
Switching Frequency (f_{sw})	50 kHz
Output Voltage (V_{out})	24 V
Current Ripple (ΔI_L)	2.184 A
Voltage Ripple (ΔV_o)	0.48 V
Inductor $L1$ and $L2$	93.4 μ H
Coupling Capacitor ($C1$)	117.87 nF
Input Capacitor (C_{in})	5460 μ F
Output Capacitor (C_{out})	235.73 μ F

2.3 GWO Algorithm

The Grey Wolf Optimizer (GWO) algorithm is inspired by the social hierarchy and hunting behavior of grey wolves. It involves initializing the social hierarchy, input data, and search agents, then iterating to find the optimal solution. Key variables such as the number of GWO agents, maximum iterations, and duty cycles are set and updated throughout the process. The stages of the algorithm include the following.

1. Tracking - Monitoring the best current solution.
2. Encircling - Updating the positions of the search agents.
3. Attacking (Exploitation) - Exploiting the best current solutions.
4. Searching (Exploration) - Exploring new areas in the search space.

To mathematically model the hunting mechanism, the GWO algorithm applies three core formulations.

1. Encircling behavior

$$\vec{D} = \vec{C} \cdot \vec{X}_{\text{leader}}(t) - \vec{X}(t) \tag{9}$$

$$\vec{X}(t+1) = \vec{X}_{\text{leader}}(t) - \vec{X}(t) \tag{10}$$

2. Coefficient vectors

$$\vec{A} = 2a \cdot r_1 - a \tag{11}$$

$$\vec{C} = 2r_2 \tag{12}$$

where $r1$ and $r2$ are random values in [0,1]. The parameter a decreases linearly from 2 to 0 during iteration to shift the balance from exploration to exploitation.

$$a = 2 - \frac{2t}{t_{\max}} \tag{13}$$

3. Position update based on the three best wolves (α, β, δ)

$$\vec{X}_1 = \vec{X}_\alpha - \vec{A}_1 \cdot |\vec{C}_1 \cdot \vec{X}_\alpha - \vec{X}| \tag{14}$$

$$\vec{X}_2 = \vec{X}_\beta - \vec{A}_2 \cdot |\vec{C}_2 \cdot \vec{X}_\beta - \vec{X}| \tag{15}$$

$$\vec{X}_3 = \vec{X}_\delta - \vec{A}_3 \cdot |\vec{C}_3 \cdot \vec{X}_\delta - \vec{X}| \tag{16}$$

The next position of each agent is computed as follows:

$$\vec{X}(t+1) = \frac{\vec{X}_1 + \vec{X}_2 + \vec{X}_3}{3} \tag{17}$$

These formulations enable the GWO algorithm to search for the optimal duty cycle by iteratively converging toward the global Maximum Power Point. The algorithm refines the power value to achieve the best MPPT performance, as detailed in Figure 5.

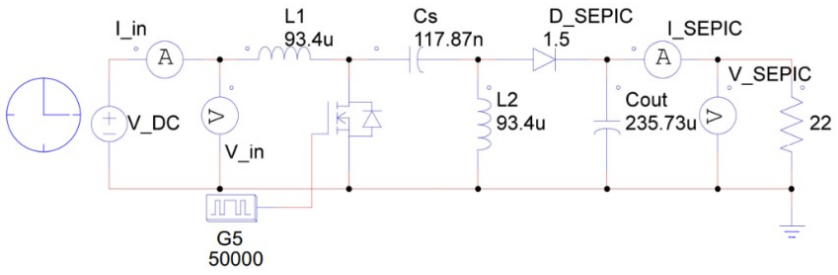

Figure 8: SEPIC configuration.

3 Results and Discussion

3.1 SEPIC Converter Performance & Test Result

This testing is conducted to assess the performance of the SEPIC Converter designed according to planning and calculations. The testing is also intended to confirm that the SEPIC Converter can be used for research purposes. The SEPIC Converter circuit used is the one that aligns with the design in Figure 8.

With the practical data obtained from the SEPIC Converter test and simulation, a comparison is made between the two datasets to calculate the resulting error. The average error calculation reveals the accuracy of the SEPIC Converter design for research purposes. Table 2 represents the comparison values between the practical and simulated test data.

The data from The SEPIC converter were evaluated through practical laboratory measurements and PSIM-based simulations to verify its suitability for MPPT applications. Table 2 presents a direct comparison between the measured and simulated output voltages in duty cycles of 58%, 62%, 65%, and 68%. Overall, the converter demonstrates a **consistent reduction in error** as the duty cycle increases. The highest average error is observed at **58% (25.45%)**, while the lowest occurs at **68% (15.26%)**. This downward trend indicates that the converter performs more accurately under a higher duty-cycle operation, aligning with the optimal operating region designed for the SEPIC topology. The error values below **20% in duty cycles** $\geq$ **and 62%** confirm that the converter meets the acceptable tolerance for MPPT research applications. Furthermore, the stable relationship between the input and output voltage at all test points suggests that the SEPIC circuit maintains predictable behavior, reinforcing its reliability for integration with real-time MPPT algorithms.

3.2 MPPT Simulation under Ideal and Non-Ideal Conditions

The purpose of this testing is to determine and ensure that the MPPT Algorithm design can function effectively and trigger the MPPT system to produce the highest Output Voltage with the designed PV panel source and converter system. The MPPT GWO Algorithm design is tested within the PSIM application on the MPPT system circuit assembled according to the initial design components. Testing is also conducted to verify that the C program can be implemented in the control system and that its algorithm can operate as intended.

Figure 9 displays the MPPT System assembled from various function blocks in such a way as to resemble the arrangement of the actual components of the MPPT system. The

Table 2: Connection of peripherals to microcontroller

No.	Duty (%)	V_{in} (V)	V_{out}(V)		Error (%)
			Practical	Simulation	
1.	58	12	8.59	11.80	27.20
2.	58	13	9.46	12.82	26.21
3.	58	14	10.23	13.84	26.08
4.	58	15	11.12	14.85	25.12
5.	58	16	11.93	15.87	24.83
6.	58	17	12.73	16.89	24.63
7.	58	18	13.60	17.91	24.06
8.	62	12	10.22	12.99	21.32
9.	62	13	11.15	14.12	21.03
10.	62	14	12.12	15.25	20.52
11.	62	15	13.04	16.37	20.34
12.	62	16	13.98	17.49	20.07
13.	62	17	14.94	18.62	19.76
14.	62	18	15.89	19.75	19.54
15.	65	12	11.63	14.03	17.11
16.	65	13	12.65	15.23	16.94
17.	65	14	13.68	16.43	16.74
18.	65	15	14.74	17.63	16.39
19.	65	16	15.82	18.83	15.99
20.	65	17	16.90	20.04	15.67
21.	65	18	18.03	21.24	15.11
22.	68	12	13.09	15.57	15.93
23.	68	13	14.22	16.91	15.91
24.	68	14	15.44	18.25	15.40
25.	68	15	16.6	19.58	15.22
26.	68	16	17.79	20.92	14.96
27.	68	17	19.00	22.26	14.65
28.	68	18	20.10	23.59	14.79

Solar Panel functions as the main power source with specifications similar to the one used. A resistor load is applied as the load for the converter output, with a value of 1820Ω for simulation to achieve voltages up to 24 V. Two conditions are applied to the Solar Panel: when the Irradiance is constant at 1000 W/m^2 and the temperature is constant at 25°C, and when the Irradiance and Temperature vary. These two conditions are applied to determine if the uploaded algorithm can work under non-ideal conditions. The component values of the converter are adjusted according to the designed configuration. In the converter, the MOSFET is connected to a specific function block provided by PSIM to upload the designed algorithm in the form of a C language.

The algorithms simulated in PSIM are the GWO Algorithm, the PnO Algorithm, and the HC Algorithm, with GWO as the main focus observed for its performance when compared to the simulation results of the other algorithms. This comparison is presented in the form of graphs for each MPPT Output resulting from the simulation when each Algorithm code is applied, and they are displayed together to observe the differences between them. The parameters controlled by each algorithm are shown in Table 3 for the three algorithms.

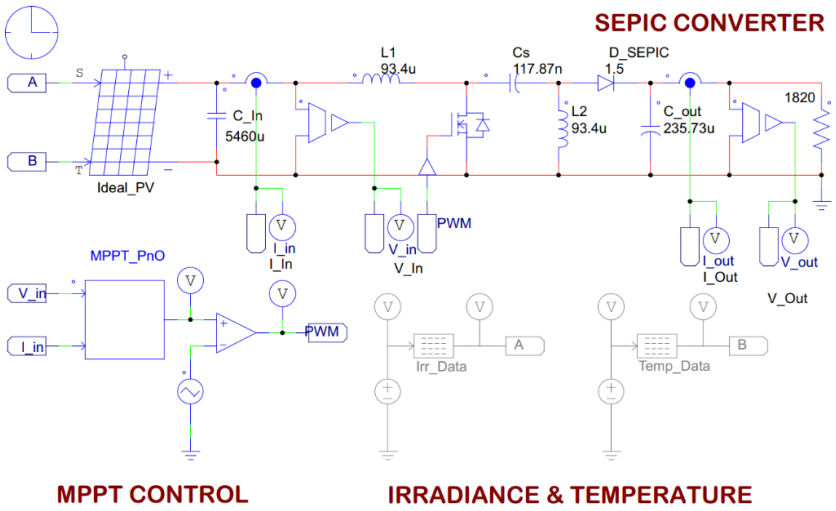

Figure 9: MPPT system configuration.

Table 3: Connection of Peripherals to Microcontroller

Perturb and Observe	Hill Climbing	Grey Wolf Optimizer
$D = 0.6$	$D = 0.6$	$N = 5$; Max_Iter = 10
$D_{\max} = 0.68$	$D_{\max} = 0.68$	$r1 = r2 = \text{rand}()/50000$
$D_{\min} = 0.58$	$D_{\min} = 0.58$	Pos_max = 0.68
Step_Duty = 0.01	Step_Duty = 0.01	Pos_min = 0.58

The parameter settings from Table 3 are used for the values of each algorithm to be used as references for the MPPT system control. For GWO, it is set that the values of $r1$ and $r2$ are adjusted so that when the program generates random values, they fall between 0 and 1. The number of GWOs is set to 5, and the optimum position as the Duty cycle solution is set with maximum and minimum values between 0.68 and 0.58, in accordance with the optimum capacity of the SEPIC converter. For the program's iterations, it is limited to 10 loops. Both the PnO and HC algorithms apply the same parameters, with an initial Duty of 0.6 and a Duty step of 0.01. The simulation of the three algorithms is performed by providing Irradiance and Temperature Profiles to the PV Panel, which is then observed for changes in its Output Voltage over a period of 1 second (1000 ms). The data is then presented in the form of a graph showing changes in Output Voltage, which is also compared with Input Voltage.

Simulation tests were conducted to validate the GWO-based MPPT algorithm against the P&O and HC methods. The MPPT system was tested under two scenarios:

1. **Ideal conditions** (irradiance 1000 W/m², temperature 25°C)
2. **Nonideal conditions** (varying irradiance and temperature profiles)

Under ideal conditions, the photovoltaic panel produces approximately 21.55 V, and MPPT algorithms adjust the duty cycle to reach an optimized output voltage of 25.56 V in

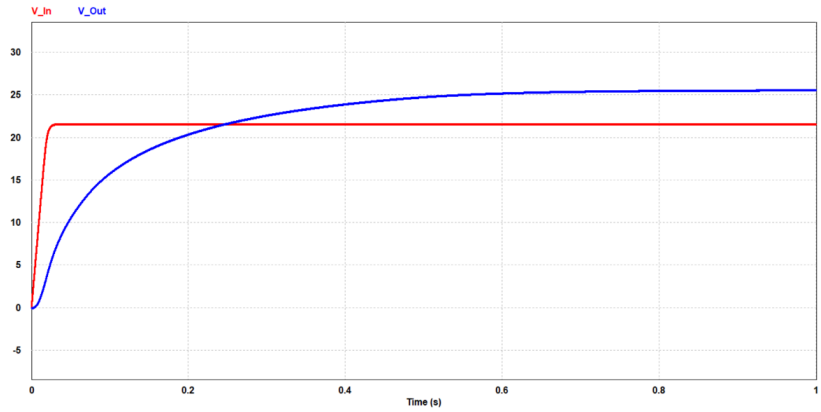

Figure 10: Input & output voltage graph for ideal condition.

1 second. The GWO algorithm converges significantly faster, reaching its optimum duty cycle in 2 ms, compared to HC (12 ms) and P&O (15 ms).

In non ideal conditions, GWO maintains robust performance, achieving 99.87% accuracy and 140 ms tracking speed. Meanwhile, P&O suffers substantial degradations, dropping to 65.35% accuracy due to oscillation and local peak trapping, an expected weakness in perturbative MPPT methods. Table 4 summarizes the superiority of GWO in accuracy, speed, and resilience.

Table 4: Connection of peripherals to microcontrollern

PV Condition	MPPT Algorithm	Optimum Power (Watt)	Tracking Speed (s)	Tracking Accuracy (%)
Ideal	P&O	34.22	0.015	99.97
	HC	35.87	0.012	99.97
	GWO	35.89	0.002	99.97
Non Ideal	P&O	30.33	0.17	65.35
	HC	31.96	0.33	98.15
	GWO	31.97	0.14	99.87

The graph shown in Figure 10 is the result of the simulation of the ideal condition of the GWO MPPT system for Input Voltage and Output Voltage. The graph also depicts the performance of the SEPIC converter design with the PV Panel as the power source and under constant Irradiance and Temperature conditions. The graph represents the results obtained when the three MPPT control algorithms are applied, with the algorithms gradually determining the Duty cycle for the converter to achieve optimal Output Voltage based on the received Input. As shown in the figure, under ideal conditions, the PV generates a voltage of approximately 21.55 V, and gradually, the algorithm selects and adjusts the Duty cycle for the converter until it achieves the optimization of the Output Voltage, reaching approximately 25.56 V within 1 second. The graph shown in Figure 11 is the result of the simulation of the GWO MPPT system under non-ideal conditions for Input Voltage and

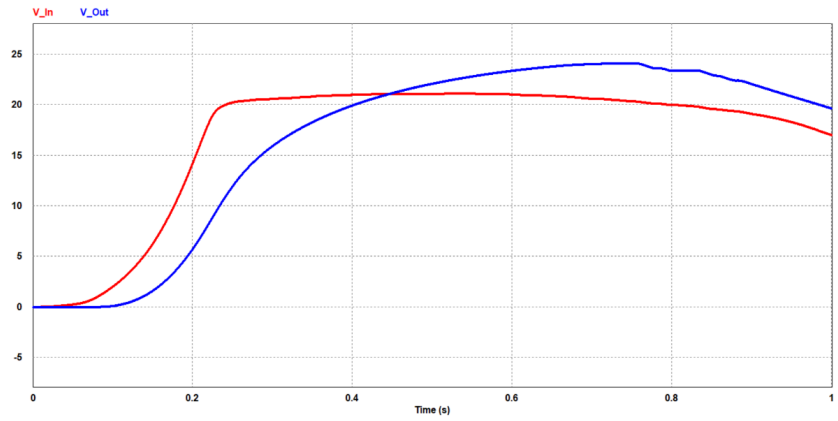

Figure 11: Input & output voltage graph for non ideal condition.

Output Voltage. From the irradiance and Temperature profiles, the PV panel generates a voltage that increases with the increase in the irradiance values, and around an Irradiance level of 350 W/m^2, the PV panel starts to produce a stable voltage. Based on this voltage pattern from the PV, the MPPT algorithm gradually selects and adjusts the Duty cycle until it optimizes the Output Voltage to approximately 24.12 V. Then, at around 0.8 seconds, both Input and Output Voltages experience a decrease due to a decrease in Irradiance values. In the simulation testing process, the three algorithms generate different MPPT responses. The code for the Grey Wolf Optimizer (GWO) algorithm uploaded to the C Blocks in PSIM results in a different MPPT selection process graph compared to the P&O, Hill Climbing, and PSO algorithms. The results of applying the P&O and Hill Climbing algorithms show similar graphs, so the comparison is made between the results of the GWO algorithm and the P&O-HC algorithm.

3.3 Comparative Analysis of Duty-Cycle Selection Patterns

Figure 12, Figure 13, and Figure 14 reveal distinct behavioral patterns among the three algorithms.

1. GWO exhibits a stochastic yet directed search due to random coefficients (r_1, r_2), allowing it to escape local maxima especially useful under shading.
2. P&O and HC maintain a smooth incremental adjustment in the duty-cycle, but this deterministic behavior limits their adaptability during rapid irradiance transitions.

The GWO output remains consistently near $D = 0.68$, indicating strong exploitation capability and effective convergence toward the global optimum of the converter.

The results obtained from the GWO algorithm testing in the MPPT system through simulation indicate the algorithm's capability to track the optimum point from the solar panel input and maximize the output power, both in ideal and non-ideal conditions. The test results also demonstrate the ability of the GWO algorithm, where compared to the P&O and HC algorithms, it can generate more optimal power with an accuracy of up to 99% and a tracking speed of up to 2 ms in ideal conditions and 140 ms in non-ideal conditions.

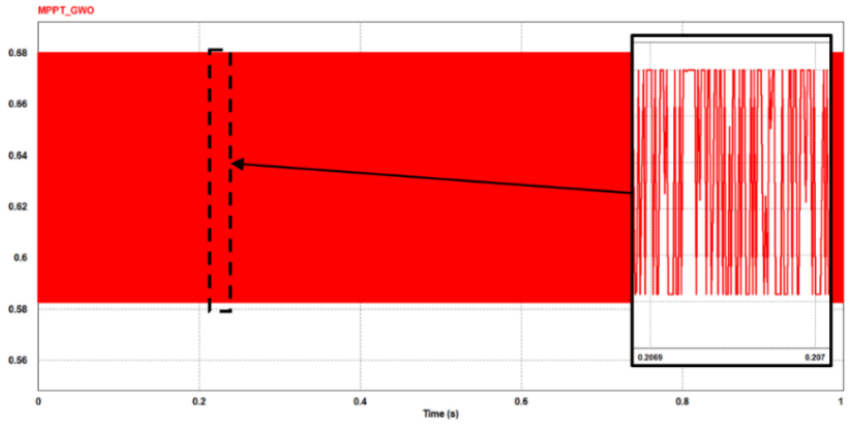

Figure 12: Duty selection of MPPT performance of GWO.

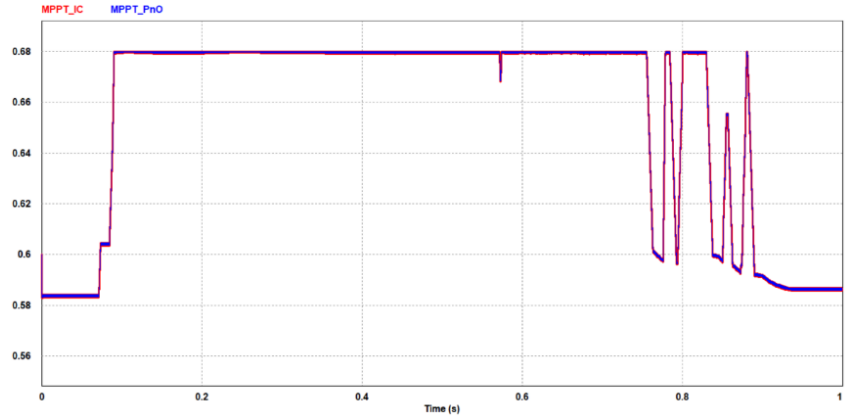

Figure 13: Duty selection of MPPT performance of P&O.

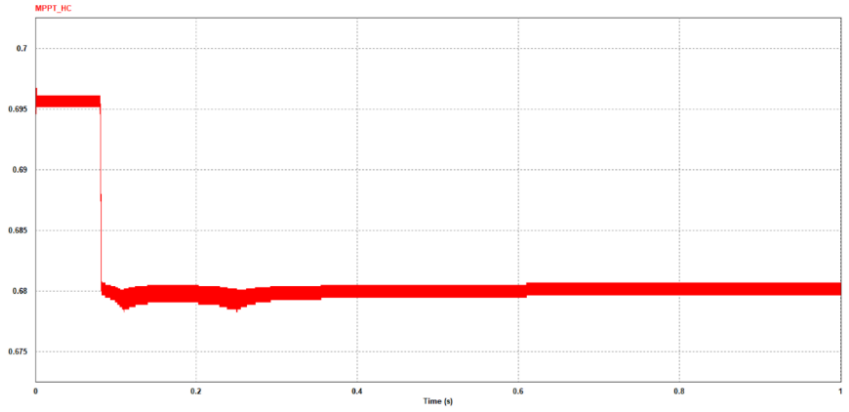

Figure 14: Duty selection of MPPT performance of HC.

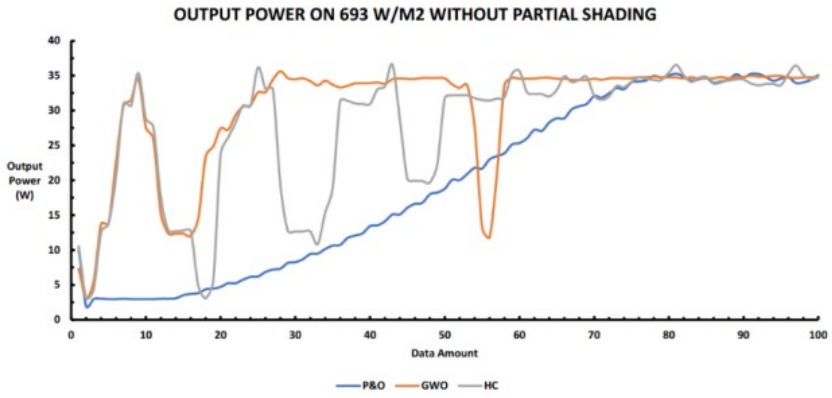

Figure 15: Output power result graph on 693 W/m^2 without partial shading.

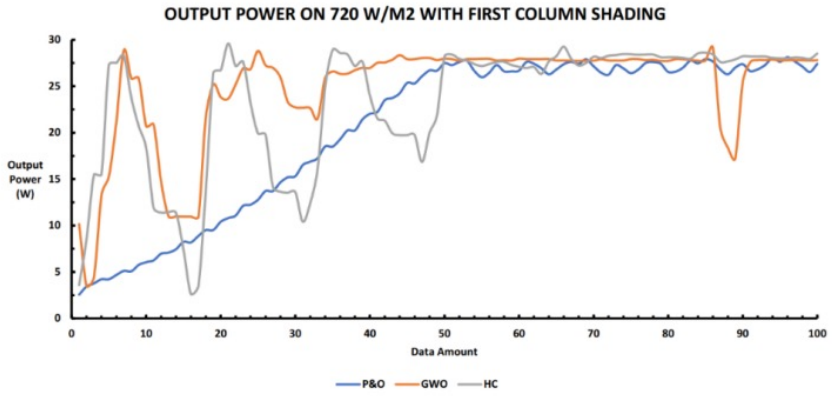

Figure 16: Output power result graph on 720 W/m^2 with first column shading.

3.4 Performance Under Partial Shading

Figure 15, Figure 16, and Figure 17 illustrate the output power of the system in three shading scenarios as follows.

1. No shading (693 W/m^2)
2. Column shading (720 W/m^2)
3. Row shading (789 W/m^2)

In all scenarios, GWO consistently generates higher peak power and exhibits less fluctuation compared to P&O and HC. This resilience under partial shading is a direct consequence of the GWO exploration mechanism, allowing it to avoid false MPPs created by multi-peak characteristics.

The results obtained from the Integration Testing of the MPPT System indicate that the MPPT System has been successfully constructed by integrating the GWO MPPT Algorithm with the SEPIC Converter. The testing results demonstrate that the system is capable of

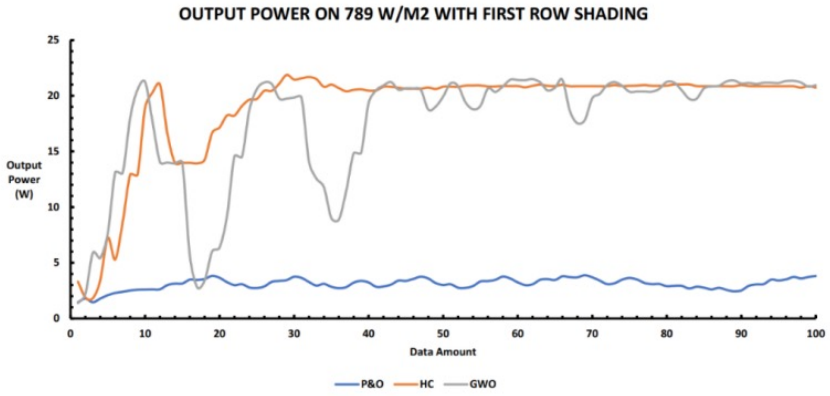

Figure 17: Output power result graph on 789 W/m^2 with first row shading.

dynamically tracking input power and can generate optimal power output under varying environmental conditions.

This testing also confirms the capability of the GWO Algorithm in terms of its optimization performance. The results from several graphs show that the GWO Algorithm is faster in tracking the optimum point and more efficient in achieving maximum power. This algorithm also exhibits better resilience and stability compared to other algorithms, as evidenced by the graphs showing that the GWO Algorithm tends to be more linear even under various environmental conditions.

4 Conclusion

The comparative evaluation between the SEPIC converter and the GWO-based MPPT algorithm reveals several significant findings beyond the primary performance indicators. First, the decreasing trend in the average error from 25.45% at a duty cycle of 58% to 15.26% at 68% indicates that the SEPIC topology not only meets its design specifications but also demonstrates stable operational behavior in a broad range of switching conditions. Second, integration testing confirms that GWO consistently maintains its convergence near the optimal duty cycle region, reflecting its strong exploitation capability compared to classical perturbative algorithms. Third, the partial shading experiments show that GWO maintains output linearity and mitigates power fluctuation more effectively, indicating a practical robustness under field-level non-uniform irradiance.

Future research may further enhance the system by:

1. integrating adaptive or self-tuning parameters in GWO to reduce dependency on fixed search-agent initialization,
2. developing a hybrid GWO–IC or GWO–PSO structure to accelerate tracking under highly dynamic irradiance,
3. implementing real-time embedded optimization on FPGA to minimize execution latency, and
4. Redesign of the SEPIC converter using coupled inductors or synchronous switching to increase overall efficiency beyond the current of 62.45%.

References

[1] R. Sulistyowati, D. C. Riawan, and M. Ashari, "Pv farm placement and sizing using ga for area development plan of distribution network," in *2016 International Seminar on Intelligent Technology and Its Applications (ISITIA)*, pp. 509–514, IEEE, 2016.

[2] J. Ahmad, F. Spertino, A. Ciocia, and P. Di Leo, "A maximum power point tracker for module integrated pv systems under rapidly changing irradiance conditions," in *2015 International Conference on Smart Grid and Clean Energy Technologies (ICSGCE)*, pp. 7–11, IEEE, 2015.

[3] P. K. Atri, P. Modi, and N. S. Gujar, "Comparison of different mppt control strategies for solar charge controller," in *2020 International Conference on Power Electronics & IoT Applications in Renewable Energy and its Control (PARC)*, pp. 65–69, IEEE, 2020.

[4] G. Dhaouadi, O. Djamel, S. Youcef, and C. Salah, "Implementation of incremental conductance based mppt algorithm for photovoltaic system," in *2019 4th International Conference on Power Electronics and their Applications (ICPEA)*, pp. 1–5, IEEE, 2019.

[5] S. Singh, S. Manna, M. I. H. Mansoori, and A. Akella, "Implementation of perturb & observe mppt technique using boost converter in pv system," in *2020 international conference on computational intelligence for smart power system and sustainable energy (CISPSSE)*, pp. 1–4, IEEE, 2020.

[6] I. Sara and R. Faulianur, "Grey wolf optimization for track maximum power of photovoltaic system in multiple peak power characteristics," in *IOP Conference Series: Materials Science and Engineering*, vol. 523, p. 012047, IOP Publishing, 2019.

[7] S. D. Nugraha, E. Wahjono, E. Sunarno, D. O. Anggriawan, E. Prasetyono, and A. Tjahjono, "Maximum power point tracking of photovoltaic module for battery charging based on modified firefly algorithm," in *2016 International Electronics Symposium (IES)*, pp. 238–243, IEEE, 2016.

[8] S. Mirjalili, S. M. Mirjalili, and A. Lewis, "Grey wolf optimizer," *Advances in engineering software*, vol. 69, pp. 46–61, 2014.

[9] S. Kigsirisin and H. Miyauchi, "Optimal power flow solutions using directive independence grey wolf optimizer," in *2021 IEEE Region 10 Symposium (TENSYMP)*, pp. 1–7, IEEE, 2021.

[10] Ł. Knypiński and L. Nowak, "Application of the grey wolf algorithm for optimization of pm synchronous motor," in *2019 19th International Symposium on Electromagnetic Fields in Mechatronics, Electrical and Electronic Engineering (ISEF)*, pp. 1–2, IEEE, 2019.

[11] S. Sukumar, M. Marsadek, A. Ramasamy, and H. Mokhlis, "Grey wolf optimizer based battery energy storage system sizing for economic operation of microgrid," in *2018 IEEE International Conference on Environment and Electrical Engineering and 2018 IEEE Industrial and Commercial Power Systems Europe (EEEIC/I&CPS Europe)*, pp. 1–5, IEEE, 2018.

[12] H. A. Sujono, R. Sulistyowati, A. Safi'i, and C. W. Priananda, "Photovoltaic farm with maximum power point tracker using hill climbing algorithm," *ARPN Journal of Engineering and Applied Sciences*, vol. 13, no. 13, pp. 4167–4172, 2018.

[13] M. Ghalambaz, R. J. Yengejeh, and A. H. Davami, "Building energy optimization using grey wolf optimizer (gwo)," *Case Studies in Thermal Engineering*, vol. 27, p. 101250, 2021.

[14] J.-S. Wang and S.-X. Li, "An improved grey wolf optimizer based on differential evolution and elimination mechanism," *Scientific reports*, vol. 9, no. 1, p. 7181, 2019.

[15] T. Patarau, S. R. Daraban, D. Petreus, and R. Etz, "A comparison between sepic and buck-boost converters used in maximum power point trackers," in *Proceedings of the 2011 34th International Spring Seminar on Electronics Technology (ISSE)*, pp. 397–402, IEEE, 2011.

[16] R. Sulistyowati, R. S. Wibowo, D. C. Riawan, and M. Ashari, "Power and voltage estimation of unobserved bus on distribution network using anfis algorithm with the modified pso-ga hybrid," *International Review of Electrical Engineering*, vol. 15, no. 6, pp. 493–501, 2020.

[17] M. Verma and S. S. Kumar, "Hardware design of sepic converter and its analysis," in *2018 International Conference on Current Trends towards Converging Technologies (ICCTCT)*, pp. 1–4, IEEE, 2018.

[18] R. Sulistyowati, "Optimum placement of measurement devices on distribution networks using integer linear k-means clustering method," *Przegląd Elektrotechniczny*, vol. 96, 2020.

[19] S. C. Krauter, *Solar electric power generation: Photovoltaic energy systems*. Springer, 2006.